Micromechanical modelling of complex shear modulus of crumb rubber modified bitumen

Wang, Haopeng; Liu, Xueyan; Zhang, Hong; Apostolidis, Panos; Erkens, Sandra; Skarpas, Athanasios

Important note
To cite this publication, please use the final published version (if applicable).
Please check the document version above.

Micromechanical modelling of complex shear modulus of crumb rubber modified bitumen

Haopeng Wang [a,*], Xueyan Liu [a], Hong Zhang [a], Panos Apostolidis [a], Sandra Erkens [a], Athanasios Skarpas [a,b]

[a] Section of Pavement Engineering, Faculty of Civil Engineering & Geosciences, Delft University of Technology, Delft, the Netherlands
[b] Department of Civil Infrastructure and Environmental Engineering, Khalifa University, Abu Dhabi, United Arab Emirates

HIGHLIGHTS

- The bitumen matrix is stiffer than neat bitumen and rubber inclusion is softer than dry rubber.
- The volume concentration of rubber increased to approximately two times after swelling from simulation.
- The predicted complex shear modulus of CRMB using micromechanical models correlated well with experimental results.

GRAPHICAL ABSTRACT
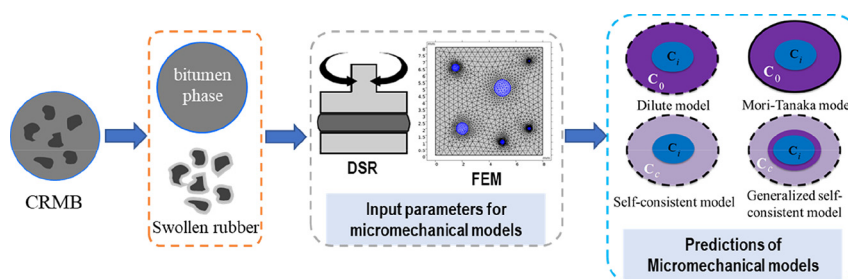
ABSTRACT

Crumb rubber modified bitumen (CRMB) can be considered as a binary composite system where rubber particles are embedded in the bitumen matrix. The bitumen-rubber interaction process (mainly swelling) significantly changes the mechanical properties of both bitumen and rubber phases. This study aims to predict the complex moduli of CRMB binders with more representative constituent parameters using micromechanical models. To achieve this goal, frequency sweep tests using a dynamic shear rheometer were performed on the liquid phase of CRMB and swollen rubber samples to represent the essential properties of bitumen matrix and rubber inclusion. In addition, the numerical swelling model was developed to estimate the effective volume concentration of rubber after swelling. Results show that the liquid phases of CRMB are stiffer and more elastic than the neat bitumen while the swollen rubber is softer and more viscous than the dry rubber. The effective volume concentration of rubber can increase to 2.126 times as the blend percentage based on the finite element analysis. Using the liquid phase of CRMB binder and swollen rubber properties as the micromechanical model inputs yield more accurate predictions. The used four micromechanical models predict well at higher frequencies while underestimating the complex modulus at lower frequencies.

1. Introduction

The utilization of crumb rubber modified bitumen (CRMB) has become a common practice in the asphalt paving industry for many years. Besides the tremendous environmental benefits, modification of bitumen with crumb rubber modifiers (CRMs) from scrap tires was reported to improve the physical and mechanical properties of binders. Comparing to neat bitumen, CRMB has a higher resistance to rutting, aging, fatigue and thermal cracking [1–3]. These improvements are attributable to the interaction between bitumen and CRM. The bitumen-rubber interaction plays an important role not only in the property

* Corresponding author.
E-mail address: haopeng.wang@tudelft.nl (H. Wang).

development of CRMB but also, in its storage, transport, and construction. Depending on different interaction parameters (e.g., temperature, time and mixing technique, etc.), there are two mechanisms involved in the bitumen-rubber interaction process: rubber particle swelling and chemical degradation (devulcanization and/or depolymerization) [4,5]. Rubber swelling in bitumen is a diffusion-induced volume expansion process of rubber particles through absorbing light fractions from bitumen [6]. Under severe interaction conditions (excessively high mixing temperature with high shear and extended mixing time), rubber network degradation may occur after achieving the swelling equilibrium. Rubber degradation is a chain disentanglement/scission process of the swollen rubber, which breaks down the polymer chain bonds or crosslinking bonds reducing thus the molecular weight of rubber [7]. The raw material parameters (e.g., bitumen microstructure and composition, rubber composition, morphology and particle size, etc.) were also reported to have great impacts on the interaction process of rubber in bitumen.

The bitumen-rubber interaction alters not only the component fractions and microstructure of bitumen but also the nature of rubber. The rubber swelling process stiffens the binder while degradation is detrimental to the mechanical properties of the binder. For the conventional wet-processed CRMB at a temperature of approximately 180 °C, only partial degradation occurs, and the final binder properties are dominated by the rubber swelling process [4]. Therefore, it is of vital importance to understand the interaction process to guide the production of CRMB.

Although considerable work has been done to measure and even predict empirical and fundamental properties of CRMB, very little work has been reported in which rigorous mechanics-based models have been used to investigate the complicated behavior of CRMB [8]. Some empirical models were developed to describe the effect of rubber particles in CRMB. These straightforward models are based on the correlations between rubber related variables (particle size, surface area, etc.) and resultant composite response [9,10], which are incapable of providing generalized insights into the impact of multi-physical interactions between the constituents. The stiffening or reinforcement mechanisms of rubber in bitumen may stem from volume-filling reinforcement, physiochemical interaction and interparticle interaction.

Micromechanical models, which can predict fundamental material properties of a composite based on mechanical properties and volume fractions of individual constituents, have been introduced to predict the effective viscoelastic behavior of asphaltic materials [11–14]. In the composite system of asphalt mastics or mixtures, fillers and aggregates are usually regarded as inert rigid materials embedded in the bitumen matrix [15]. CRMB can be regarded as a binary composite in which bitumen is the matrix while rubber particles are the inclusions. However, unlike asphalt mastic or mixture, the composite system of CRMB is more complicated due to the interaction between rubber particles and bitumen which changes both the mechanical properties and volume fractions of individual constituents. In general, bitumen-rubber interaction (mainly swelling) has three consequences from a micromechanics-based point of view: (1) changing the component proportions and thus the mechanical properties of bitumen matrix due to the absorption of light fractions by rubber; (2) changing the mechanical properties of rubber due to the formation of a gel-like structure; (3) changing the effective volume content of rubber due to the volume expansion [5]. Therefore, the accurate determination of input parameters from constituents would be a challenge and directly influence the accuracy of the model prediction. The predictions of mechanical properties of CRMB from the known properties and blend percentages of the constituent phases enable a more appropriate selection of source materials (bitumen and rubber type), enhanced material development (binder preparation conditions) and improved design of binders (rubber content and particle gradation).

Among different micromechanical models, the following four models are considered as more representative and well-known

[12,14]: the dilute model (DM), the Mori-Tanaka model (MTM), the self-consistent model (SCM), the generalized self-consistent model (GSCM). These models were used in this study to predict the complex shear modulus of CRMB.

2. Objective and approach

This study aims to predict the complex shear modulus of CRMB with different rubber contents using four common micromechanical models. To achieve this goal, the following subtasks were done to obtain accurate input parameters for micromechanical models:

- Frequency sweep tests using dynamic shear rheometer (DSR) were conducted on neat bitumen and CRMB binders with four different rubber contents. The obtained complex modulus data are compared with the model predicted values to examine the performance of different micromechanical models.
- Frequency sweep tests were conducted on both extracted liquid phases of CRMBs and swollen rubber samples to obtain more representative rheological properties of bitumen matrix and rubber inclusion in the composite system of CRMB.
- Finite element method was employed to estimate the volume change of rubber in bitumen after swelling thus to obtain the effective volume content of rubber in CRMB.

After obtaining the input parameters for micromechanical models, they were implemented into different micromechanical models to predict the complex modulus. The predicted results were then compared with the experimental data. An overview of the research steps taken in this study is presented in Fig. 1.

3. Micromechanical models

3.1. Homogenization concept

Homogenization theory was developed to estimate the effective properties of a heterogeneous composite based on the microstructural description and the local behaviors of its constituents. In this theory, a representative volume element (RVE) is chosen to represent the overall properties of the composite. In an RVE of the CRMB composite system, the constitutive equations of each phase (bitumen and rubber) are shown in Eqs. (1a) and (1b). The average stress and strain of the composite can be related to the average stress and strain of each phase in combination with each volume fraction in Eqs. (1c) and (1d).

$$\langle \boldsymbol{\sigma} \rangle_b = \mathbf{C}_b : \langle \boldsymbol{\varepsilon} \rangle_b \tag{1a}$$

$$\langle \boldsymbol{\sigma} \rangle_r = \mathbf{C}_r : \langle \boldsymbol{\varepsilon} \rangle_r \tag{1b}$$

$$\langle \boldsymbol{\sigma} \rangle_c = (1-\phi)\langle \boldsymbol{\sigma} \rangle_b + \phi \langle \boldsymbol{\sigma} \rangle_r \tag{1a}$$

$$\langle \boldsymbol{\varepsilon} \rangle_c = (1-\phi)\langle \boldsymbol{\varepsilon} \rangle_b + \phi \langle \boldsymbol{\varepsilon} \rangle_r \tag{1d}$$

where $\langle \boldsymbol{\sigma} \rangle$, $\langle \boldsymbol{\varepsilon} \rangle$ are the average stress and strain; $\mathbf{C}$ is the stiffness tensor; ϕ is the volume fraction of rubber phase; the subscripts "b", "r" and "c" represent the bitumen phase, rubber phase, and CRMB composite respectively. Considering the relationship between $\langle \boldsymbol{\sigma} \rangle_c$ and $\langle \boldsymbol{\varepsilon} \rangle_c$, the effective stiffness tensor of the composite $\mathbf{C}_c$ can be defined as

$$\langle \boldsymbol{\sigma} \rangle_c = \mathbf{C}_c : \langle \boldsymbol{\varepsilon} \rangle_c \tag{2}$$

To calculate the effective stiffness tensor, a strain localization tensor **A** is introduced to relate the homogenized strain tensor to the local
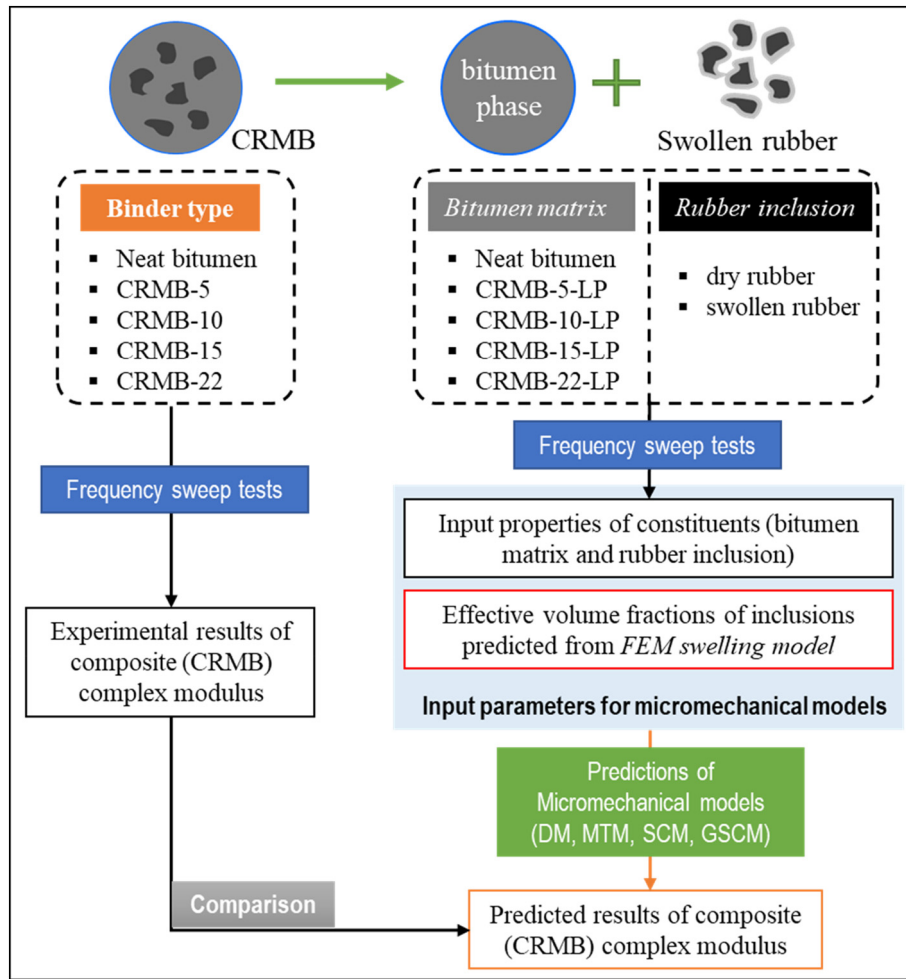
Fig. 1. Flowchart of research steps in this study.

strain tensor in Eqs. (3a) and (3b).

$$\langle \boldsymbol{\varepsilon} \rangle_b = \mathbf{A}_b : \langle \boldsymbol{\varepsilon} \rangle_c \quad (3a)$$

$$\langle \boldsymbol{\varepsilon} \rangle_r = \mathbf{A}_r : \langle \boldsymbol{\varepsilon} \rangle_c \quad (3b)$$

It is easy to find the strain localization tensor of each phase has the following relationship with the corresponding volume fraction:

$$(1-\phi)\mathbf{A}_b + \phi \mathbf{A}_r = \mathbf{I} \quad (4)$$

where $\mathbf{I}$ is the unit fourth-order tensor. The key point of the homogenization process is to obtain the strain localization tensor that once known, the effective stiffness tensor of the composite $\mathbf{C}_c$ can be calculated by combining Eqs. (1a, 1b, 1c, 1d)–(4) as

$$\mathbf{C}_c = \mathbf{C}_b + \phi(\mathbf{C}_r - \mathbf{C}_b) : \mathbf{A}_r \quad (5)$$

Various micromechanical models were developed to calculate the localization tensor $\mathbf{A}$ based on Eshelby's pioneering work on elastic solutions for a spherical or elliptical inclusion being embedded in an infinite matrix [16,17]. The elastic theory used here can be extended to viscoelastic materials according to the elastic-viscoelastic correspondence principle [18]. The following sections will introduce four micromechanical models in the context of the CRMB composite system.

3.2. Dilute model

In the dilute model (DM), particles are embedded in an infinite matrix that the particle interactions can be disregarded due to the dilute distribution of particles. The strain localization tensor of rubber can be directly obtained from the Eshelby's solution:

$$\mathbf{A}_r^{\text{DM}} = \left[\mathbf{I} + \mathbf{S}_b : (\mathbf{C}_b)^{-1} : (\mathbf{C}_r - \mathbf{C}_b) \right]^{-1} \quad (6)$$

where $\mathbf{S}_b$ is the Eshelby's tensor obtained from the properties of the bitumen matrix.

3.3. Mori-Tanaka model

In the Mori-Tanaka model (MTM), each particle is embedded in a matrix with a uniform strain the same as the average strain of the matrix [19]. Therefore, the interactions between inclusions are considered. The strain localization tensor of rubber can be calculated from the dilute model:

$$\mathbf{A}_r^{\text{MT}} = \mathbf{A}_r^{\text{DM}} : \left[(1-\phi)\mathbf{I} + \phi \mathbf{A}_r^{\text{DM}} \right]^{-1} \quad (7)$$

3.4. Self-consistent model

In the self-consistent model (SCM), each inclusion is assumed to be embedded in an infinite homogenous medium whose mechanical

properties are the same as the composite [20]. The strain localization tensor of rubber is expressed as:

$$\mathbf{A}_r{}^{SC} = \left[\mathbf{I} + \mathbf{S}_c : (\mathbf{C}_c)^{-1} : (\mathbf{C}_r - \mathbf{C}_c)\right]^{-1} \qquad (8)$$

where $\mathbf{S}_c$ is the Eshelby's tensor obtained from the properties of CRMB composite. It is noted that the effective stiffness tensor $\mathbf{C}_c$ is implicitly given when calculating it. Therefore, it needs to be solved using a recursive method by assuming an initial value equal to that of the matrix.

3.5. General self-consistent model

The general self-consistent model (GSCM) assumes a spherical particle embedded in a spherical annulus of the matrix material, which in turn is embedded in an infinite medium with the effective mechanical properties of the composite. The effective shear modulus of the composite G_c follows a quadratic equation:

$$A\left(\frac{G_c}{G_b}\right)^2 + 2B\left(\frac{G_c}{G_b}\right) + C = 0 \qquad (9)$$

where G_b is the shear modulus of the tumen matrix. A, B, and C are related to the mechanical properties and volume fraction of each phase. The detailed formulations of these parameters can be found elsewhere [21].

4. Materials and method

4.1. Materials and binder preparation

Penetration grade 70/100 bitumen (Nynas) commonly used in the Netherlands was served as the base bitumen in this study. The SARA (saturates, aromatics, resins, and asphaltenes) fractions of the base bitumen are 7%, 51%, 22%, and 20% respectively (Iatroscan TLC-FID). The density of bitumen is 1.03 g/cm³. The ambient ground CRMs from waste truck tires have an irregular shape and particle sizes ranging from 0 to 0.71 mm. The basic properties, composition and particle gradation of CRM are shown in Table 1. The processing agents mainly consist of antioxidants/antiozonants and curing additives (e.g., sulfur, zinc oxide, stearic acid, accelerator and oil etc.).

The CRMB binders were produced in the laboratory by blending different percentages of CRMs with base bitumen. Four CRM contents including 5%, 10%, 15% and 22% by mass of base bitumen were used. These CRMBs were labeled as CRMB-5, CRMB-10, CRMB-15 and CRMB-22. Manual stirring for 5 min was applied to pre-distribute

Table 1
Basic properties and particle size distribution of CRM.

Properties		Description or value	
Source		Scrap truck tires	
Colour		Black	
Morphology		Porous	
Specific gravity (g/cm³)		1.15	
Decomposition temperature (°C)		~200	
Chemical composition	Total rubber (natural and synthetic)	55	
	Carbon black (%)	25	
	Processing agents (%)	20	
Gradation	Sieves (mm)	Passing (%)	Retained (%)
	0.710	100	0
	0.500	93	7
	0.355	63	30
	0.180	21	42
	0.125	9	12
	0.063	2	7
	Pan	–	2

CRMs into base bitumen, then the blend was mixed using a Silverson high shear mixer with a square hole screen at 180 °C with the shearing speed of 6000 rpm for 30 min. This mixing condition was optimized based on the criteria to obtain better mechanical properties of CRMB [5]. During the laboratory mixing process, the mixing head was immersed into the hot bitumen to avoid vortex which may involve the potential oxidative aging.

4.2. Extraction of liquid phase of CRMB

To obtain the mechanical properties of the bitumen matrices of CRMB binders, the liquid phase of CRMB was extracted by removing the insoluble CRM particles from the bitumen matrix. In this regard, the required amount of fresh CRMB binders was heated to 165 °C and drained through a mesh sieve (0.063 mm) in the oven at 165 °C for 20 min [22]. To allow for a fast and uniform filtration, the heated CRMB samples were manually flattened on the mesh before the drainage. The residual (drained) binder designated as CRMB-X-LP (X represents the rubber content) was collected on an aluminum pan. The extracted liquid phase was stored in the refrigerator immediately to prevent any unwanted aging or reaction and was subjected to DSR testing later.

4.3. Preparation of swollen rubber sample

The cylindrical rubber samples were cut from waste truck tires as shown in Fig. 2. A uniform rubber slice of 2 mm thickness was cut from the tire tread (metal fiber free) using the water jet cutting technology. Then, laser cutting was applied on the slice to obtain the rubber cylinders with a diameter of 8 mm. These cylindrical rubber samples (2 mm-thickness and 8 mm-diameter) were subjected to the swelling test at 180 °C for 36 h. Based on previous studies [23], the rubber sample is believed to reach the swelling equilibrium after 36 h immersion in the hot bitumen at 180 °C. The swollen rubber samples were cleaned from bitumen by wiping with absorbent paper while hot and brushing for a few seconds with cold trichloroethylene gently. All the samples were brushed until there were no significant bitumen imprints left on the white absorbent paper. Through this process, the sample consistency was controlled. The obtained swollen rubber sample is a gel-like material with light-fractions inside the rubber network. Since the geometry of cylindrical rubber samples changed after swelling, a special drill tool with an inner diameter of 8 mm was used to trim the swollen sample into the desired diameter. A fast punching force was applied to eliminate the creep deformation of swollen rubber samples at room temperature. No absorbed bitumen was squeezed out of rubber. DSR tests were performed on both dry (unswollen) and swollen rubber samples.

4.4. Dynamic shear rheometer test

A dynamic shear rheometer (Anton Paar) was utilized to obtain the rheological parameters (complex shear modulus and phase angle) of both binder samples and rubber samples following the standard test method. Frequency sweep tests of CRMB and liquid phase binder samples were carried out with a parallel-plate geometry (25 mm diameter and 1 mm gap) from 0.1 to 100 rad/s at temperatures of 10, 30, 50 and 70 °C. Before the frequency sweep tests, strain amplitude sweep tests were conducted to identify the linear viscoelastic (LVE) range and all the measurements were carried out at a strain level of 0.1% under strain-controlled mode.

The mechanical properties of rubber before and after swelling were tested by DSR using the 8-mm parallel plates. The unreacted (dry) cylindrical rubber sample can be directly placed between the parallel plates of the DSR. Before the placement, a special glue was applied on the surface of the bottom plate and the top surface of the rubber sample. Excess glue was removed. The test started after the hardening of glue to a
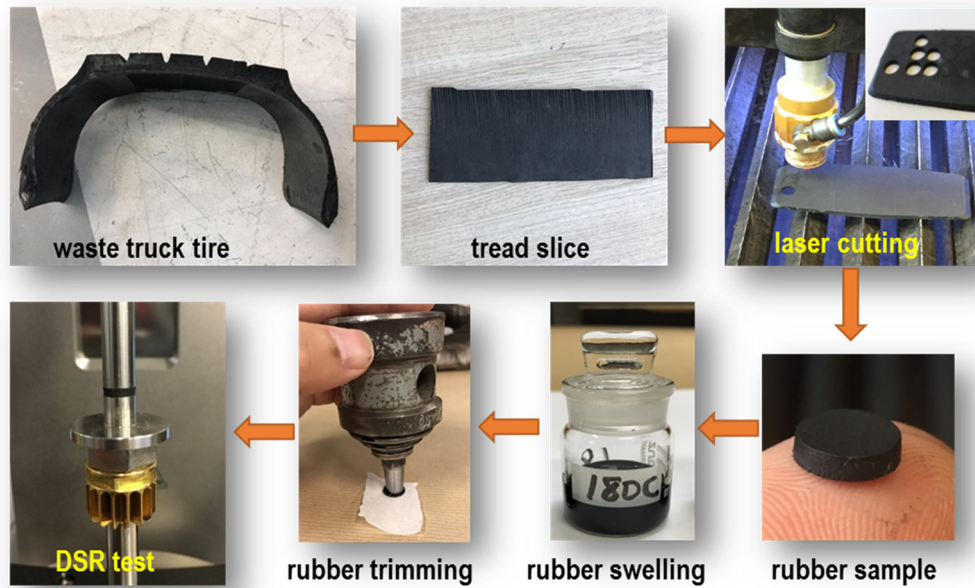
Fig. 2. Preparation of cylindrical dry rubber and swollen rubber samples.

proper bonding between rubber and plates. Due to the good adhesion between the plates and swollen rubber, no glue was used. For both dry and swollen rubber samples, a manual adjustment was applied to the gap between the plates until the normal force is close to zero. Frequency sweep tests of rubber samples were performed from 0.1 to 100 rad/s over a temperature range of −10–130 °C with an increment of 20 °C. According to the previous study, the measurements were carried out at a strain level of 1% under strain-controlled mode [24]. The viscoelastic parameters (complex modulus and phase angle) of each sample were collected and analyzed.

5. Results and discussion

5.1. Effect of CRM content on the rheology of CRMB

In the present study, a modified Christensen-Anderson-Marasteanu (CAM) model (Eqs. (10) and (11)) and Williams-Landel-Ferry (WLF) equation (Eq. (12)) for shift factors fitting were used to develop complex modulus and phase angle master curves of binders based on the frequency sweep test results [25].

$$G^* = \frac{G_g^*}{\left[1 + (f_c/f_r)^k\right]^{m/k}} \tag{10}$$

where $G_g^* = G^*$ (f → ∞), glass complex modulus; f_c = crossover frequency at which the elastic component is approximately equal to the viscous component; f_r = reduced frequency, a function of both temperature and strain; and k, m = shape parameters, dimensionless.

$$\delta = 90I - \frac{90I - \delta_m}{\left\{1 + \left[\frac{\log(f_d/f_r)}{R_d}\right]^2\right\}^{m_d/2}} \tag{11}$$

where δ_m = phase-angle constant at f_d, the value at the inflection for binders; f_r = reduced frequency; f_d = location parameter with dimensions of frequency, at which δ_m occurs; R_d, m_d = shape parameters;

and for binders, $I = 0$ if $f > f_d$, $I = 1$ if $f \leq f_d$.

$$\log\alpha_T(T) = \frac{-C_1(T - T_R)}{C_2 + (T - T_R)} \tag{12}$$

where C_1, C_2 = empirically determined constants; T = test temperature; T_R = reference temperature; $\alpha_T(T)$ = shifting factor.

The complex modulus and phase angle master curves of CRMB binders at different rubber contents are presented in Fig. 3. As expected, the addition of CRM into bitumen improves the binder viscoelastic response. At low frequencies (corresponding to high temperatures), CRMB binder is stiffer than neat bitumen and more elastic, while at high frequencies (corresponding to low temperatures), CRMB binder is softer than neat bitumen. It is noteworthy that phase angles of all the binders merged together when approaching the high-frequency range. This because at high frequencies (low temperatures), bitumen plays a dominant role in contributing to the viscous effect of binder. The stiffening or softening extent is intensified as the CRM content increases. The phase angle master curves of all CRMB binders show the characteristic plateau in the intermediate frequency domain. This unique feature represents the presence of polymer (rubber) in the bitumen.

5.2. Input parameters for micromechanical models

5.2.1. Rheological properties of bitumen matrix and rubber inclusion

As mentioned above, the nature of both bitumen and rubber phases changed after the bitumen-rubber interaction. Therefore, it is of vital importance to measure the representative rheological properties of actual bitumen matrix and rubber inclusion in the CRMB system.

The complex modulus and phase angle master curves of the liquid phases of CRMB binders, which are considered as the actual bitumen matrices, are presented in Fig. 4. It can be seen that the liquid phases of CRMB binders are stiffer and more elastic than the neat bitumen as reflected by the increased complex modulus and decreased phase angle. With the increase of rubber content, the improvement of the viscoelasticity of the liquid phase of CRMB is more obvious. At higher rubber content, more light fractions of bitumen were absorbed by rubber particles during the interaction process, which in turn increases the proportions of asphaltenes. The asphaltenes were reported to be primarily
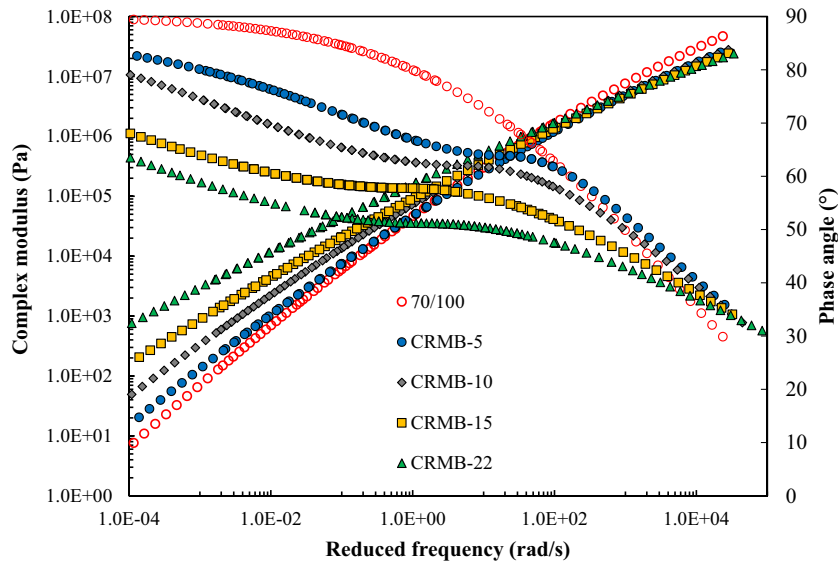
Fig. 3. Complex modulus and phase angle master curves of CRMB binders with different CRM contents at the reference temperature of 30 °C.

responsible for the increase of stiffness and elasticity [26]. Besides, with the current extraction method, micro rubber particles (smaller than 0.063 mm) may be released into the liquid phase and thus stiffen the liquid phase.

From the frequency sweep test data, it was found that rubber is not a rheologically simple material so that common rheological models for bitumen are not suitable for it. Therefore, the master curves were established using a generalized logistic function in Eq. (13) [27] and the Williams-Landel-Ferry (WLF) equation (Eq. (12)) for shift factors fitting to form smooth curves.

$$\log A = \delta + \frac{\alpha}{\left[1 + \lambda e^{(\beta + \gamma(\log \omega))}\right]^{1/\lambda}} \qquad (13)$$

where A is either complex shear modulus or phase angle. δ is the lower asymptote; α is the difference between the values of upper and lower asymptote; λ, β and γ define the shape between the asymptotes and the location of the inflection point. Based on the time-temperature superposition principle, the master curves of complex modulus and

phase angle of dry and swollen rubber samples at a reference temperature of 30 °C were built in Fig. 5.

It can be seen that dry rubber exhibits obvious elastic behaviors whose complex modulus and phase angle are almost frequency independent. However, rubber after swelling shows obvious viscoelasticity. The complex moduli of swollen rubber were lower than the dry rubber in the low-frequency range. At high frequencies, the moduli of them crossed. At the dry state, rubber polymer chains are entangled or crosslinked to each other, forming tightly folded coils, which contributes to the rubber elasticity [28]. When the rubber polymer chain segments start to absorb bitumen molecules, the folded polymer coils start unfolding, causing the swelling and loosening of the network [29]. Consequently, this polymer network swelling process will decrease the complex modulus at a macroscopic scale.

From the previous results, it is obvious that the actual bitumen matrix and rubber inclusion are significantly different from the neat bitumen and dry rubber, respectively. It is important to obtain the representative complex modulus data to be served as the input parameters for the micromechanical models in order to have more accurate predictions.
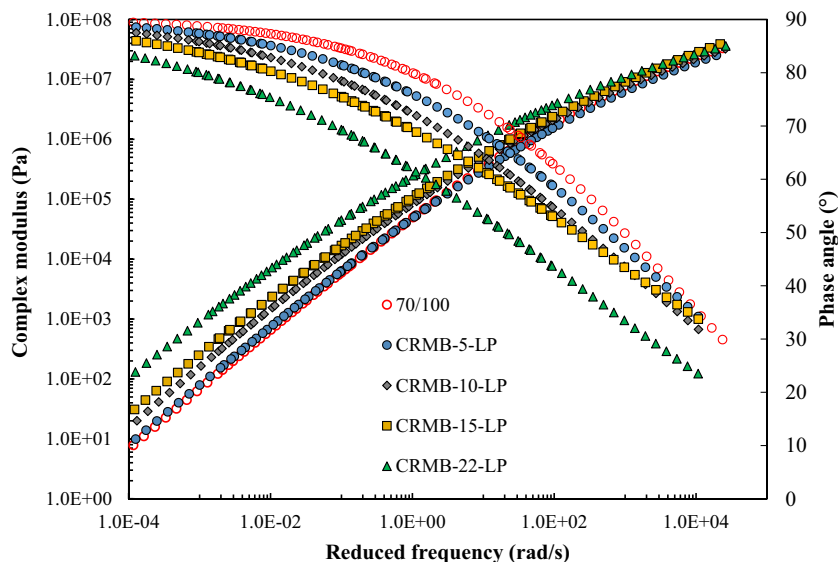

Fig. 4. Complex modulus and phase angle master curves of bitumen matrices at the reference temperature of 30 °C.
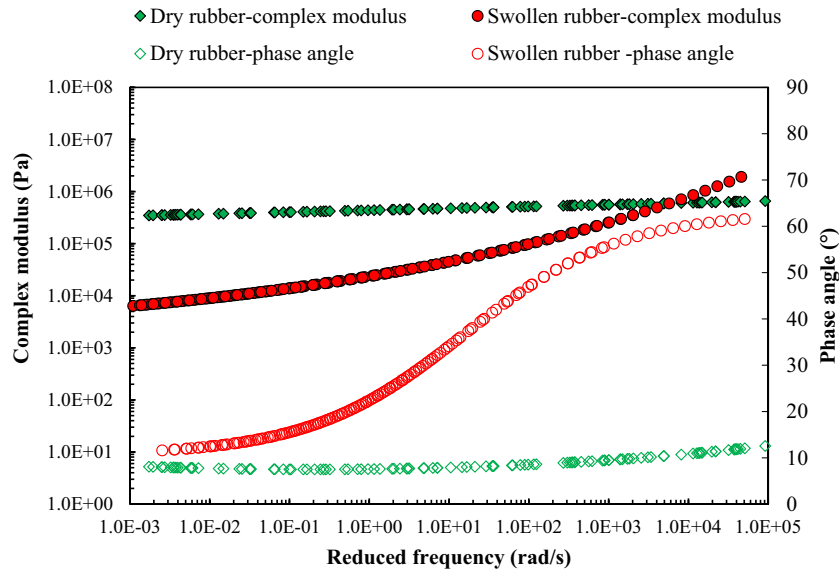
Fig. 5. Complex modulus and phase angle master curves of rubber inclusions at the reference temperature of 30 °C.

5.2.2. Estimation of effective volume content of rubber in CRMB

An important step in micromechanical modelling is to identify the effective volume content of inclusion to ensure an accurate prediction of mechanical properties. As pointed out by many studies, rubber particles experience volume expansion during the interaction process. How to quantify the precise volume increase remains a challenge. Due to the ambiguity of boundaries between bitumen and rubber phases after interaction in the binder, it is difficult and expensive to use scanning electron microscopy or X-ray computed tomography to evaluate the volume change of rubber particles [30]. Besides, it is unreasonable to assume a unified swelling ratio for all rubber particles in the binder since rubber particles of different sizes may have different swelling status and thus swelling ratios. Therefore, this study proposed a finite element method to estimate the effective volume content of rubber in CRMB. A finite element model capable of simulating the multiphysics swelling phenomenon was developed in a previous study [6]. It is the diffusion of light fractions of bitumen into rubber polymer network that causes the swelling. The rubber swelling phenomenon essentially consists of mass diffusion and volume expansion (mechanical deformation). The essential theories for mass diffusion and large deformations based on the balance equations driving the solvent diffusion and the force equilibrium, and the constitutive equations for rubber particles are presented here [6]. Eqs. (14a) and (14b) are Fick's first and second laws respectively, which describe the kinetics of bitumen diffusion into rubber.

$$\boldsymbol{J} = -D\nabla C \tag{14a}$$

$$\frac{\partial C}{\partial t} = D\nabla^2 C \tag{14b}$$

where $\boldsymbol{J}$ is the diffusion flux vector; D is the diffusion coefficient; C is the concentration; t is time; ∇ is the nabla operator or gradient operator. For the volume expansion of rubber, the equilibrium equation of motion was derived based on Newton's second law, as shown in Eq. (15a). Eq. (15b) shows the kinematic equation in terms of displacement. The total deformation gradient tensor $\mathbf{F}$ was multiplicatively decomposed into elastic and inelastic (swelling) components (Eq. (15c)).

$$\nabla \cdot \mathbf{FS} + \mathbf{F_v} = 0 \tag{15a}$$

$$\mathbf{F} = \nabla \mathbf{u} + \mathbf{I} \tag{15b}$$

$$\mathbf{F} = \mathbf{F}_{el}\mathbf{F}_{inel} \tag{15c}$$

where $\mathbf{S}$ is the second Piola-Kirchhoff stress; $\mathbf{F_v}$ is the volume force vector; $\mathbf{u}$ is the displacement; $\mathbf{I}$ is the identity tensor; $\mathbf{F}_{el}$ is the undamaged elastic deformation tensor; $\mathbf{F}_{inel}$ is the inelastic deformation tensor. A linear elastic constitutive model was used for rubber as shown in Eq. (16a). Obviously, the nonlinearity issues of rubber particles during the swelling process were not considered for simplicity. With the relationship between Cauchy stress $\boldsymbol{\sigma}$ and second Piola-Kirchhoff stress $\mathbf{S}$, Eq. (16a) can be rewritten into Eq. (16b) by involving the determinant of inelastic deformation tensor J_{in}.

$$\boldsymbol{\sigma} = \mathbf{C} : \mathbf{E}_{el} \tag{16a}$$

$$\mathbf{S} = J_{in}\mathbf{F}_{inel}^{-T}(\mathbf{C} : \mathbf{E}_{el})\mathbf{F}_{inel}^{-1} \tag{16b}$$

where $\boldsymbol{\sigma}$ and $\mathbf{E}_{el}$ are the Cauchy stress tensor and strain tensor respectively; $\mathbf{C}$ is the constitutive elasticity tensor. The mass diffusion domain was coupled with the structural deformation domain by the following equations.

$$\boldsymbol{\varepsilon}_s = \boldsymbol{\beta}_s C_{diff} \tag{17a}$$

$$\mathbf{F}_{el} = \mathbf{F}J_{in}^{-1/3} \tag{17b}$$

where $\boldsymbol{\varepsilon}_s$ is the inelastic strain caused by swelling; C_{diff} is the concentration difference; $\boldsymbol{\beta}_s$ is the swelling coefficient. The above equations were implemented to the finite element model to study the diffusion-induced volume expansion phenomenon of rubber in bitumen. The model can predict the swelling ratio of rubber particles of different sizes given the type of bitumen and rubber as well as the interaction temperature. The simulation results were validated by the experimental results [6]. The following procedures were followed to calculate the effective rubber volume.

- *Step 1*: Particle size grouping. Based on the gradation of CRM used in this study, the rubber particles were separated into six groups according to the sieve size (Fig. 6). Since the particle size distribution retained on a sieve usually follows a standard Gaussian distribution, the rubber particles retained on a certain sieve are assumed to have the same size equal to the average size of the passing sieve and retaining sieve. For instance, 7% of rubber particles retained on the
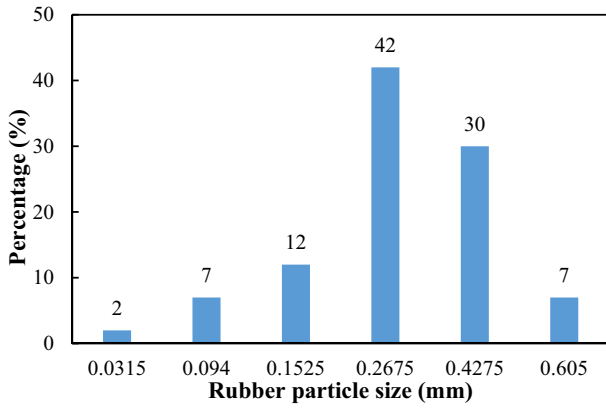
Fig. 6. The discrete particle size distribution of CRM.

0.5-mm sieve are assumed to have a uniform size of $(0.71 + 0.5)/2 = 0.605$ mm.

- *Step 2*: Finite element model development. A square two-dimensional domain of 8×8 mm meshed with triangular elements was built. Six spherical rubber particles of different sizes in step 1 were embedded in a bitumen matrix as shown in Fig. 7a. Plane strain conditions were assumed in the lateral mesh directions and no flux was imposed. The initial solvent concentration within the rubber was set as zero, which is the strain-free reference concentration. The periphery boundaries of the rubber particle contacted directly to the bitumen were set to have the same concentration as the surrounding bitumen matrix (Fig. 7b). Based on the laboratory tests on the materials used in this study, the following model input parameters were used [23]. The equilibrium swelling concentration is 628.14 kg/m^3. The diffusion coefficient of bitumen into rubber at 180 °C is 3.787×10^{-11} m^2/s. The swelling coefficient of rubber at 180 °C is 5.584×10^{-11} m^3/kg.

- *Step 3*: Numerical study analysis. The simulation results including the diffusion and deformation fields of swelling of rubber particles with six different sizes at 1800 s (corresponding to the mixing time of 30 min in this study) are presented in Fig. 8a and b. It can be seen from the concentration contour that small particles (0.0315, 0.094, 0.1525 and 0.2675 mm) are fully saturated with bitumen molecules while big particles (0.4275 and 0.605 mm) still have a concentration gradient along the direction from outer to inner. The particle size

influences the diffusion process and hence the swelling equilibrium.

- *Step 4*: Swelling ratio calculation. The black circle in Fig. 8b represents the original rubber size. Based on the area change of the rubber circle during swelling in the 2D domain, the swelling ratio, defined as the swelling area at time t divided by the original area ($t = 0$), was plotted in Fig. 9. Swelling of rubber particles occurred faster at the earlier stage and then slowed down. Small particles reached the swelling equilibrium in very short times while it took more time for big particles to reach the equilibrium. The swelling ratios of rubber particles of different sizes at 1800 s were captured from the graph and summarized in Fig. 10. Combining with the particle size distribution percentage in Fig. 6, the total effective volume content of rubber V_{eff} can be calculated using the following equation.

$$V_{eff} = \phi \cdot \sum_{i=1}^{n} p_i \cdot s_i \qquad (18)$$

where ϕ is the original volume fraction of rubber in the binder; p_i is the percentage of the ith particle size group based on the sieve size; s_i is the swelling ratio corresponding to the ith particle size; n is the total number of representative particle size. The original volume contents of rubber in CRMB-5, CRMB-10, CRMB-15, CRMB-22 are 4.29%, 8.22%, 11.84% and 16.46% respectively. The corresponding effective volume contents of rubber estimated by the above method are 9.11%, 17.47%, 25.18%, and 34.99% respectively. The weighted averaged swelling ratio of rubber in CRMB is approximately 2.126. The estimated volume contents of rubber will be implemented in the micromechanical models in the following section.

5.3. Comparison of different micromechanical models

As mentioned before, micromechanical models can predict the mechanical properties of a composite based on mechanical properties and volume fractions of individual constituents. With the obtained complex shear moduli of bitumen matrix and rubber inclusion as well as the effective volume concentration of rubber, the complex shear moduli of CRMB can be predicted using different micromechanical models. The Poisson's ratios of rubber phase and bitumen phase were assumed to be 0.45 and 0.49, respectively [31]. For comparison purposes, the predicted complex moduli of CRMB from different micromechanical
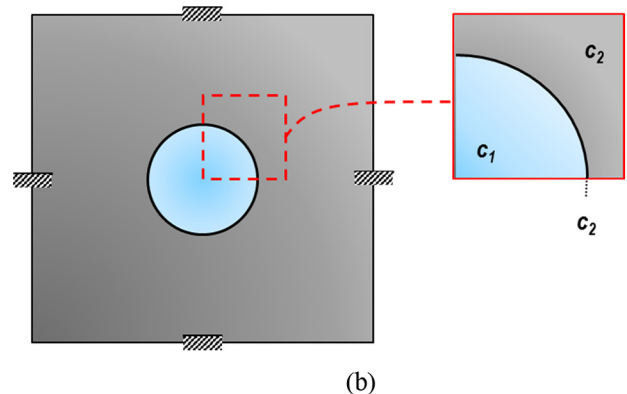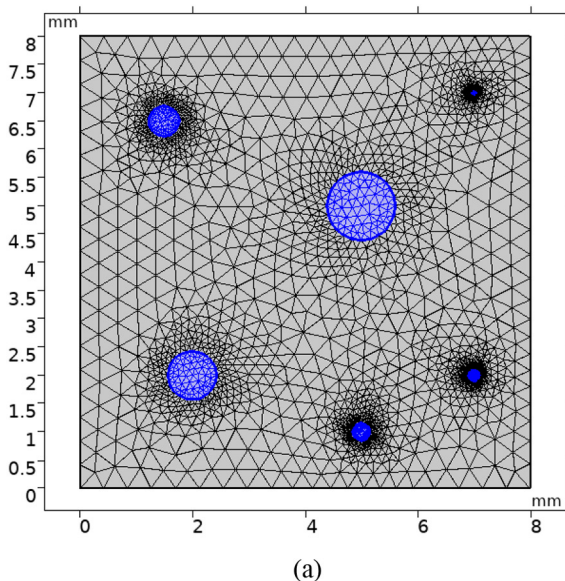

Fig. 7. (a) Geometry and mesh of the modelling domain: multiple rubber particles of varying sizes; (b) Schematic plot of boundary conditions.
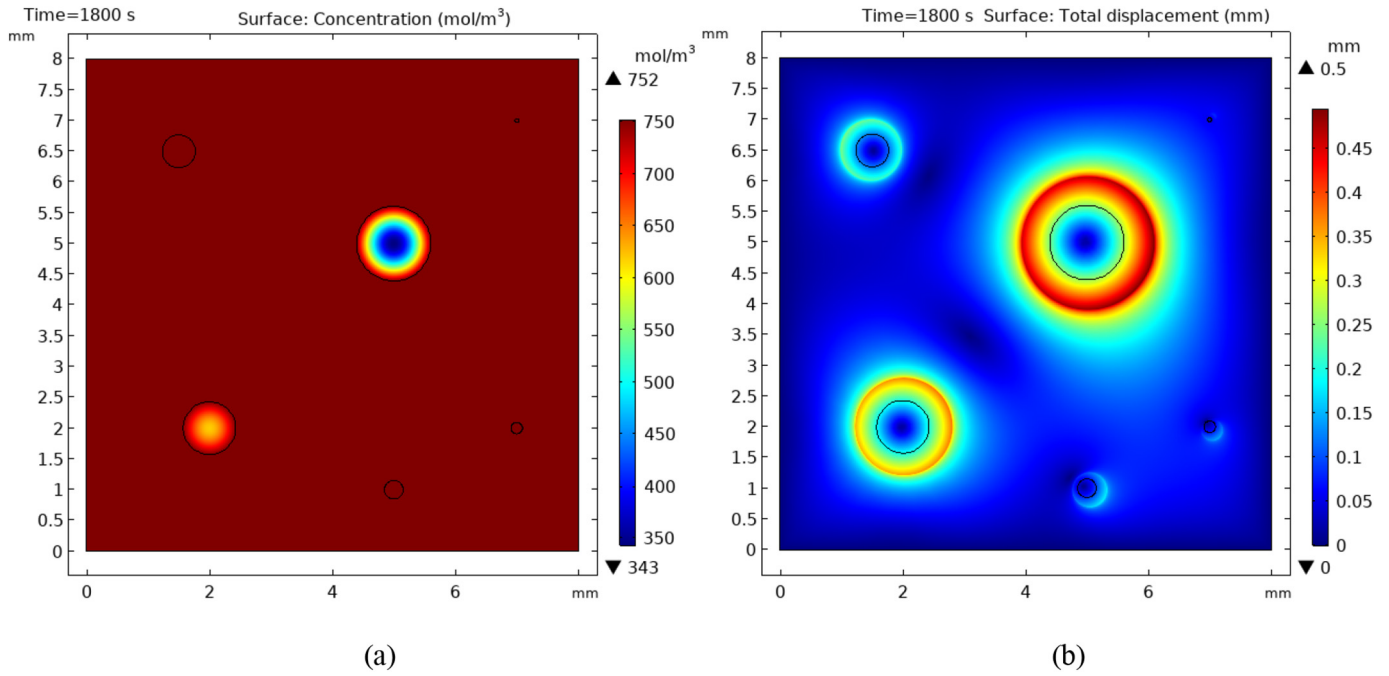
(a)

(b)

Fig. 8. Simulation results of rubber swelling in bitumen at 180 °C: (a) concentration and (b) total displacement of rubber particles at t = 1800 s.

models using both original and calibrated constituent parameters as the inputs were presented in Figs. 11 and 12 respectively. The original constituent parameters mean the mechanical properties of neat bitumen and dry rubber, and the initial volume fraction of rubber without considering the swelling effect. The calibrated constituent parameters mean the mechanical properties of liquid-phase bitumen and swollen rubber and the effective volume fraction of rubber considering the swelling effect. It can be found from Fig. 10 that most of the rubber particles have reached the swelling equilibrium while for the large rubber particles, a swelling gradient exists from the outer layer to the inner core of rubber. This means the large rubber particle (unsaturated) is not a uniform continuum. However, for simplicity, all the rubber particles here adopted the mechanical properties of the swollen rubber obtained through the DSR tests as the calibrated input mechanical parameters for the micromechanical models. The multilayer structure of certain large rubber particles will be considered for future research using models like (n + 1)- phase GSC model [32].

From Fig. 11, it can be seen that when the volume concentration of rubber is low (CRMB-5 in Fig. 11a), the predicted complex moduli from models are quite close to the experimental values. This is because

the models are more dependent on the matrix properties and the bitumen matrix property was not influenced significantly by rubber at low concentrations. With the increase of rubber concentration, the model predicted results started to deviate from the experimental data. The deviation became more obvious at high concentrations. This essentially demonstrates that using the original constituent properties will yield biased predictions from the micromechanical models.

In contrast, using the calibrated constituent parameters of CRMB yield more accurate complex modulus predictions as shown in Fig. 12. While all the micromechanical models perform well at low rubber concentrations, biased complex moduli were predicted at high rubber concentrations. This would be the same reason as explained before. For CRMB with high rubber contents, all the models still yield accurate predictions in the high-frequency range while they underestimated the complex modulus in the low-frequency range. Among the four models, MTM, SCM, and GSCM yield similar predictions but GSCM has the highest prediction accuracy. The DM overestimated the complex modulus in the middle-frequency range for all the four CRMB binders, especially at high rubber concentrations. This stems from the initial assumption of DM which ignores the particle interactions. It is known that the low-frequency range corresponds to the high-temperature
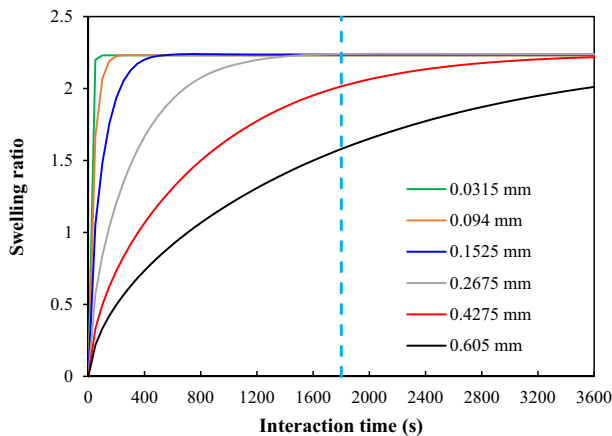

Fig. 9. Swelling ratio evolution with time of different sized particles.
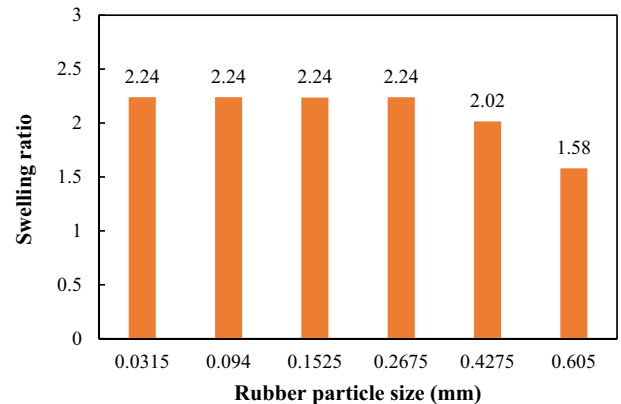

Fig. 10. The swelling ratios of rubber particles of different sizes at 1800 s.

range in the master curve frame. The rubber particles will be more active in CRMB at high temperatures since the bitumen phase is softer. The underestimation of complex modulus at high temperatures may be originated from the fact that the current models cannot capture the interparticle interactions. At high temperatures, the CRMB system behaves like a colloidal suspension system. The mechanical difference between bitumen matrix and rubber inclusion becomes larger as can be seen in Fig. 5. Interparticle interactions including hydrodynamic interaction and colloidal forces play more important roles in determining the mechanical response of the composite system [33].

To sum up, micromechanical models using the calibrated constituent parameters yield much more accurate predictions of complex modulus of CRMB than the original parameters do. All the micromechanical models give reasonable predictions when the rubber concentration is low. However, when increasing the rubber content, micromechanical models yield biased predictions in the low-frequency range. This is associated with the fact these models are primarily developed to account for the stiffening effect resulting from the embedded inclusions in a matrix with minimal or limited particle interactions, which is the case of dispersed suspensions [12,14]. Under this circumstance, the behavior of the suspension is dominated by the matrix phase. Therefore, to remedy the underestimation of complex modulus of CRMB at lower frequencies, the interparticle interactions need to be addressed in future studies. Previous studies have given an approximate analytical solution for the pairwise inter-particle interaction in a two-phase composite with

highly concentrated and randomly located spherical particles [34]. A conditional probability function can be introduced to account for the probabilistic pairwise particle interaction effects from near-field particles in the matrix [35].

6. Conclusions and recommendations

This study aimed to predict the complex modulus of CRMB with more representative constituent parameters. Frequency sweep tests using DSR were performed on both binders and individual constituents (bitumen matrix and rubber inclusion). Finite element method was used to estimate the effective volume concentration of rubber. The following conclusions can be drawn:

- The liquid phases of CRMB binders (real bitumen matrices) are stiffer and more elastic than the neat bitumen as reflected by the increased complex modulus and decreased phase angle.
- Dry rubber exhibits obvious elastic behaviors whose complex modulus and phase angle are almost frequency independent. Swelling significantly alters the rubber properties, making it softer and more viscous.
- The volume concentration of rubber increased to 2.126 times as the blend percentage estimated from the numerical swelling model.
- Using the liquid phase of CRMB binder and swollen rubber properties as the micromechanical model inputs yield more accurate predictions.
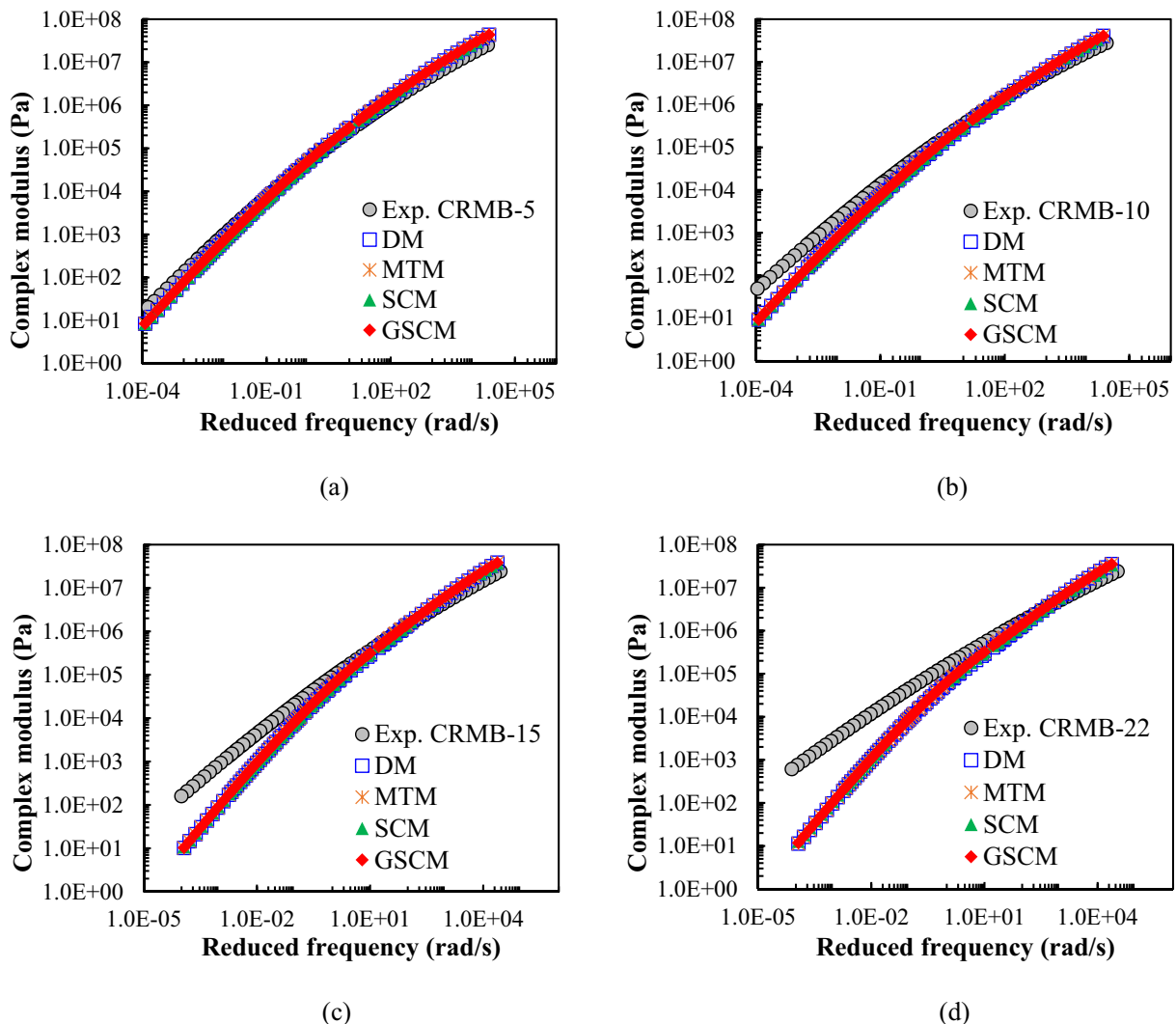

(a)

(b)

(c)

(d)

Fig. 11. Micromechanical model predicted complex moduli of CRMB using the original constituent parameters.
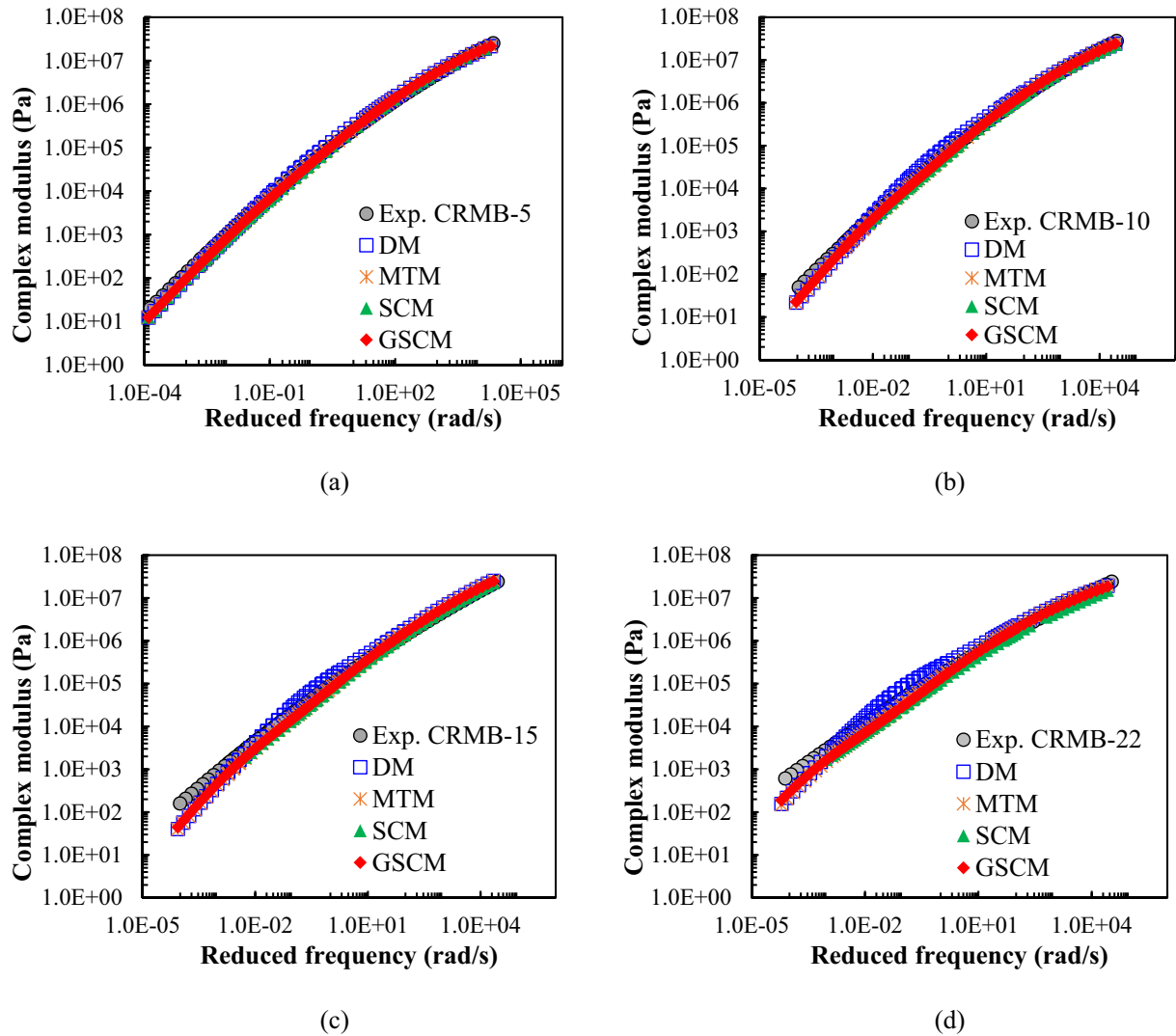
Fig. 12. Micromechanical model predicted complex moduli of CRMB using the calibrated constituent parameters.

The used four micromechanical models predict well at higher frequencies while underestimating the complex modulus at lower frequencies. Among the four used models, GSCM has the highest prediction accuracy.

Ongoing X-ray CT scan tests on CRMB samples are expected to obtain the real volume contents of swollen rubber and to be compared with the simulated results. Future studies should be undertaken to investigate the multilayer structure of swollen rubber particles as well as the interparticle interactions in CRMB in order to amend the current micromechanical models to have more accurate predictions.

CRediT authorship contribution statement

Haopeng Wang: Conceptualization, Investigation, Methodology, Writing - original draft, Writing - review & editing.**Xueyan Liu:**Investigation, Supervision.**Hong Zhang:**Methodology, Visualization.**Panos Apostolidis:**Investigation, Methodology.**Sandra Erkens:**Funding acquisition, Project administration, Supervision.**Athanasios Skarpas:**Funding acquisition, Project administration, Supervision.

Declaration of competing interest

The authors declare that they have no known competing financial interests or personal relationships that could have appeared to influence the work reported in this paper.

Acknowledgments

Data availability

The raw/processed data required to reproduce these findings cannot be shared at this time as the data also forms part of an ongoing study.

References

[1] D. Lo Presti, Recycled tyre rubber modified bitumens for road asphalt mixtures: a literature review, Constr. Build. Mater. 49 (2013) 863–881.
[2] X. Shu, B.S. Huang, Recycling of waste tire rubber in asphalt and portland cement concrete: an overview, Constr. Build. Mater. 67 (2014) 217–224.

[3] H. Wang, X. Liu, P. Apostolidis, T. Scarpas, Review of warm mix rubberized asphalt concrete: towards a sustainable paving technology, J. Clean. Prod. 177 (2018) 302–314.
[4] M.A. Abdelrahman, S.H. Carpenter, Mechanism of the interaction of asphalt cement with crumb rubber modifier, Transp. Res. Rec. 1661 (1999) 106–113.
[5] H. Wang, X. Liu, H. Zhang, P. Apostolidis, T. Scarpas, S. Erkens, Asphalt-rubber interaction and performance evaluation of rubberised asphalt binders containing non-foaming warm-mix additives, Road Mater. Pavement Des. (2018) 1–22.
[6] H. Wang, X. Liu, P. Apostolidis, S. Erkens, T. Scarpas, Numerical investigation of rubber swelling in bitumen, Constr. Build. Mater. 214 (2019) 506–515.
[7] L. Zanzotto, G. Kennepohl, Development of rubber and asphalt binders by depolymerization and devulcanization of scrap tires in asphalt, Transp. Res. Rec. 1530 (1996) 51–58.
[8] J.R. Medina, B.S. Underwood, Micromechanical shear modulus modeling of activated crumb rubber modified asphalt cements, Constr. Build. Mater. 150 (2017) 56–65.
[9] J. Shen, S. Amirkhanian, F. Xiao, B. Tang, Influence of surface area and size of crumb rubber on high temperature properties of crumb rubber modified binders, Constr. Build. Mater. 23 (1) (2009) 304–310.
[10] J. Shen, S. Amirkhanian, F. Xiao, B. Tang, Surface area of crumb rubber modifier and its influence on high-temperature viscosity of CRM binders, Int. J. Pavement Eng. 10 (5) (2009) 375–381.
[11] W. Buttlar, D. Bozkurt, G. Al-Khateeb, A. Waldhoff, Understanding asphalt mastic behavior through micromechanics, Transp. Res. Rec. 1681 (1999) 157–169.
[12] H.M. Yin, W.G. Buttlar, G.H. Paulino, H.D. Benedetto, Assessment of existing micromechanical models for asphalt mastics considering viscoelastic effects, Road Mater. Pavement Des. 9 (1) (2008) 31–57.
[13] B.S. Underwood, Y.R. Kim, A four phase micro-mechanical model for asphalt mastic modulus, Mech. Mater. 75 (2014) 13–33.
[14] H. Zhang, K. Anupam, A. Scarpas, C. Kasbergen, Comparison of different micromechanical models for predicting the effective properties of open graded mixes, Transp. Res. Rec. 2672 (28) (2018) 404–415.
[15] X. Shu, B. Huang, Micromechanics-based dynamic modulus prediction of polymeric asphalt concrete mixtures, Compos. Part B 39 (4) (2008) 704–713.
[16] J. Eshelby, The elastic field outside an ellipsoidal inclusion, Proc. R. Soc. London A Math. Phys. Eng. Sci. R. Soc. (1959) 561–569.
[17] J.D. Eshelby, The determination of the elastic field of an ellipsoidal inclusion, and related problems, Proc. R. Soc. London A Math. Phys. Eng. Sci. R. Soc. (1957) 376–396.
[18] Z. Hashin, Complex moduli of viscoelastic composites—I. General theory and application to particulate composites, Int. J. Solids Struct. 6 (5) (1970) 539–552.
[19] T. Mori, K. Tanaka, Average stress in matrix and average elastic energy of materials with misfitting inclusions, Acta Metall. 21 (5) (1973) 571–574.
[20] R. Hill, A self-consistent mechanics of composite materials, J. Mech. Phys. Solids 13 (4) (1965) 213–222.
[21] R. Christensen, K. Lo, Solutions for effective shear properties in three phase sphere and cylinder models, J. Mech. Phys. Solids 27 (4) (1979) 315–330.
[22] D. Wang, D. Li, J. Yan, Z. Leng, Y. Wu, J. Yu, H. Yu, Rheological and chemical characteristic of warm asphalt rubber binders and their liquid phases, Constr. Build. Mater. 193 (2018) 547–556.
[23] H. Wang, X. Liu, P. Apostolidis, S. Erkens, A. Skarpas, Experimental investigation of rubber swelling in bitumen, Transp. Res. Rec. (2020)(In press).
[24] A. Zegard, F. Helmand, T. Tang, K. Anupam, A. Scarpas, Rheological properties of tire rubber using dynamic shear rheometer for fem tire-pavement interaction studies, 8th International Conference on Maintenance and Rehabilitation of Pavements, Research Publishing Services, Singapore 2016, pp. 535–544.
[25] H. Wang, X. Liu, P. Apostolidis, T. Scarpas, Rheological behavior and its chemical interpretation of crumb rubber modified asphalt containing warm-mix additives, Transp. Res. Rec. 2672 (28) (2018) 337–348.
[26] J.C. Petersen, R. Glaser, Asphalt oxidation mechanisms and the role of oxidation products on age hardening revisited, Road Mater. Pavement Des. 12 (4) (2011) 795–819.
[27] G. Rowe, G. Baumgardner, M. Sharrock, Functional forms for master curve analysis of bituminous materials, Advanced Testing and Characterisation of Bituminous Materials, vols 1 and 2, , 2009 , (81–+).
[28] J.E. Mark, Rubber elasticity, J. Chem. Educ. 58 (11) (1981) 898–903.
[29] H. Wang, P. Apostolidis, J. Zhu, X. Liu, A. Skarpas, S. Erkens, The role of thermodynamics and kinetics in rubber-bitumen systems: a theoretical overview, Int. J. Pavement Eng. (2019)(In press).
[30] M.E. Kutay, S. Varma, A. Jamrah, A micromechanical model to create digital microstructures of asphalt mastics and crumb rubber-modified binders, Int. J. Pavement Eng. 18 (9) (2015) 754–764.
[31] Q. Aurangzeb, H. Ozer, I.L. Al-Qadi, H.H. Hilton, Viscoelastic and Poisson's ratio characterization of asphalt materials: critical review and numerical simulations, Mater. Struct. 50 (1) (2016).
[32] E. Herve, A. Zaoui, N-layered inclusion-based micromechanical modelling, Int. J. Eng. Sci. 31 (1) (1993) 1–10.
[33] T. Tadros, Interparticle interactions in concentrated suspensions and their bulk (rheological) properties, Adv. Colloid Interf. Sci. 168 (1–2) (2011) 263–277.
[34] J.W. Ju, T.M. Chen, Effective elastic moduli of two-phase composites containing randomly dispersed spherical inhomogeneities, Acta Mech. 103 (1994) 123–144.
[35] J.W. Ju, K. Yanase, Micromechanics and effective elastic moduli of particle-reinforced composites with near-field particle interactions, Acta Mech. 215 (1–4) (2010) 135–153.